ELSEVIER

Journal of Power Sources 112 (2002) 41–48

JOURNAL OF POWER SOURCES

www.elsevier.com/locate/jpowsour

Layered $Li(Ni_{0.5-x}Mn_{0.5-x}M'_{2x})O_2$ ($M' = Co$, Al, Ti; $x = 0$, 0.025) cathode materials for Li-ion rechargeable batteries

S.-H. Kang[a], J. Kim[a], M.E. Stoll[a], D. Abraham[a], Y.K. Sun[b], K. Amine[a,*]

[a]*Electrochemical Technology Program, Chemical Technology Division, Argonne National Laboratory, 9700 South Cass Avenue Building 203-C110, Argonne, IL 60439, USA*

[b]*Division of Chemical Technology, Hanyang University, Seoul 133-791, South Korea*

Received 13 May 2002

Abstract

Layered $Li(Ni_{0.5-x}Mn_{0.5-x}M'_{2x})O_2$ materials ($M' = Co$, Al, Ti; $x = 0$, 0.025) were synthesized using a manganese-nickel hydroxide precursor, and the effect of dopants on the electrochemical properties was investigated. $Li(Ni_{0.5}Mn_{0.5})O_2$ exhibited a discharge capacity of 120 mAh/g in the voltage range of 2.8–4.3 V with a slight capacity fade up to 40 cycles (0.09% per cycle); by doping of 5 mol% Co, Al, and Ti, the discharge capacities increased to 140, 142, and 132 mAh/g, respectively, and almost no capacity fading was observed. The cathode material containing 5 mol% Co had the lowest impedance, 47 Ω cm^2, while undoped, Ti-doped, and Al-doped materials had impedance of 64, 62, and 99 Ω cm^2, respectively. Unlike the other dopants, cobalt was found to improve the electronic conductivity of the material. Further improvement in the impedance of these materials is needed to meet the requirement for powering hybrid electric vehicle (HEV, <35 Ω cm^2). In all materials, structural transformation from a layered to a spinel structure was not observed during electrochemical cycling. Cyclic voltammetry and X-ray photoelectron spectroscopy (XPS) data suggested that Ni and Mn exist as Ni^{2+} and Mn^{4+} in the layered structure. Differential scanning calorimetry (DSC) data showed that exothermic peaks of fully charged $Li_{1-y}(Ni_{0.5-x}Mn_{0.5-x}M'_{2x})O_2$ appeared at higher temperature (270–290 °C) than $LiNiO_2$-based cathode materials, which indicates that the thermal stability of $Li(Ni_{0.5-x}Mn_{0.5-x}M'_{2x})O_2$ is better than those of $LiNiO_2$-based cathode materials.

Keywords: Lithium-ion rechargeable battery; Cathode materials; Lithium manganese nickel oxides; Layered structure

1. Introduction

Due to high cost of $LiCoO_2$, a commonly used cathode material in commercial rechargeable lithium batteries, much effort has been made to develop cheaper cathode materials than $LiCoO_2$. To this end, $LiNiO_2$ and $LiMnO_2$ have been studied extensively as possible alternatives to $LiCoO_2$ [1–6]. Although there has been a lot of progress in making these materials comparable to $LiCoO_2$ in many aspects, they still possess various problems for practical applications. Stoichiometric $LiNiO_2$ is known to be difficult to synthesize and its multi-phase reactions during electrochemical cycling lead to structural degradation [1,2]. Thermal safety concerns are another issues for $LiNiO_2$ in the charged state [7,8]. To overcome the difficulties of synthesis and structural instability during cycling and to improve thermal safety, substitution of various metal ions (e.g. Mg, Co, Al, Mn, Ti, etc.) for Ni has been tried [7–11]. Layered $LiMnO_2$ has a significant drawback in its crystallographic transformation to spinel structure during electrochemical cycling [12,13]. Although layered $LiMnO_2$ materials that do not convert to spinel during cycling were reported by Paulsen et al. [14], preparation of the materials involved a cost-adding, multi-step process of ion exchange of sodium manganese bronze with lithium.

Recently, a concept of a one-to-one solid state mixture of $LiNiO_2$ and $LiMnO_2$, i.e. $Li(Ni_{0.5}Mn_{0.5})O_2$, was adopted by Ohzuku and Makimura [15] to overcome the disadvantages of $LiNiO_2$ and $LiMnO_2$, and the electrochemical cycling behavior of the $Li(Ni_{0.5}Mn_{0.5})O_2$ was proven to be superior to the end members: $Li(Ni_{0.5}Mn_{0.5})O_2$ had the same crystallographic structure as $LiCoO_2$ and $LiNiO_2$ (space group $R\bar{3}m$) and showed excellent cycleability with stable discharge capacity of ca. 130 mAh/g between 2.5 and 4.3 V with no indication of spinel formation during electrochemical cycling. However, although the idea of making a one-to-one solid solution of $LiNiO_2$ and $LiMnO_2$ worked successfully, the real feature of $Li(Ni_{0.5}Mn_{0.5})O_2$ seems to be different from

* Corresponding author. Tel.: +1-630-252-3838; fax: +1-630-972-4451.
E-mail address: amine@cmt.anl.gov (K. Amine).

0378-7753/02/$ – see front matter
PII: S0378-7753(02)00360-9

what Ohzuku and Makimura intended in terms of the oxidation states of Ni and Mn according to Lu et al. [16], who explained the electrochemical behavior of $Li[Ni_xLi_{(1/3-(2x)/3)}Mn_{(2/3-x/3)}]O_2$ ($x = 1/3$, 5/12, 1/2) on the basis of Ni^{2+} and Mn^{4+} (i.e. $Li(Ni_{0.5}{}^{2+}Mn_{0.5}{}^{4+})O_2$ for $x = 1/2$).

The reports by Ohzuku and Makimura [15] and Lu et al. [16] sparked our interest in adopting $Li(Ni_{0.5}Mn_{0.5})O_2$ as a cathode material for rechargeable lithium-ion batteries for high power hybrid electric vehicle (HEV) applications because the material is anticipated to be a cheaper and a thermally safer cathode material than the $LiCoO_2$- and $LiNiO_2$-based materials. However, $Li(Ni_{0.5}Mn_{0.5})O_2$ shows a rather small capacity in the normal operating voltage range and our preliminary studies revealed that the $Li(Ni_{0.5}Mn_{0.5})O_2$ showed rather high impedance, which is one of the most limiting factors in HEV applications. In this work, layered $Li(Ni_{0.5-x}Mn_{0.5-x}M'_{2x})O_2$ ($M' = Co$, Al, Ti; $x = 0$, 0.025) materials have been prepared using the manganese-nickel hydroxide precursor with the respective dopant; the effect of dopants on the electrochemical properties, impedance, and thermal safety was then investigated. Furthermore, X-ray photoelectron spectroscopy (XPS) and temperature-dependent magnetic moment measurements were conducted to determine oxidation states of Ni and Mn in the layered structures.

2. Experimental

$Li(Ni_{0.5-x}Mn_{0.5-x}M'_{2x})O_2$ ($M' = Co$, Al, Ti; $x = 0$, 0.025) were prepared using appropriate amounts of $LiOH{\cdot}H_2O$, manganese-nickel hydroxide (OMG, Mn:Ni = 0.50), $Co(OH)_2$, $Al(OH)_3$, and TiO_2. The starting materials were mixed in acetone using zirconia balls; the mixed powders were calcined at 600 °C for 16 h and then at 1000 °C for 15 h in air. Phase purity of the synthesized materials was established by powder X-ray diffraction (XRD).

Cyclic voltammetry and galvanostatic charge/discharge cycling were conducted with 2032-type coin cells (20 mm diameter, 3 mm thick) that were prepared in a dry room. The positive electrode consisted of 82 wt.% metal oxide powder, 10 wt.% carbon, and 8 wt.% polyvinylidene difluoride (PVDF) binder on aluminum foil. The negative electrode was either metallic lithium or graphite on copper foil. The electrolyte was 1 M $LiPF_6$ in a 1:1 mixture of ethylene carbonate (EC)/diethyl carbonate (DEC); the separator was Celgard 2500. The coin cells were galvanostatically cycled in the 2.8–4.3 V range at a current density of 0.1 mA/cm^2 at room temperature; cyclic voltammetry was carried out at sweep rates of 50–100 μV/s in the 2.5–5 V range.

XPS and magnetic susceptibility measurements were conducted on $Li(Ni_{0.5}Mn_{0.5})O_2$ samples to determine the oxidation states of Ni and Mn. XPS spectra were obtained using a Kratos Axis ULTRA X-ray Photoelectron Spectrometer under UHV conditions; the magnetic moment was measured using a Quantum Design PMMS magnetometer between 5 and 300 K using a 0.1 T applied field. In XPS, the energy of photoelectrons ejected when the sample is irradiated by soft X-rays (usually Al Kα) was analyzed. Monochromatic Al Kα (1486 eV) radiation was the primary excitation source in our experiments. Peak fits of all spectra were performed using the Shirley background correction and Gaussian–Lorentzian curve fits. The energy scale was adjusted based on the graphite peak in the C 1s spectrum at 284.5 eV.

Differential scanning calorimetry (DSC) experiments were conducted on $Li(Ni_{0.5-x}Mn_{0.5-x}M'_{2x})O_2$ samples charged to 4.3 V (versus metallic Li). The data were acquired using a Perkin-Elmer Pyris1 DSC at a scan rate of 10 °C/min in the temperature range of 50–350 °C. Commercial (Perkin-Elmer), hermetically sealed, high-pressure titanium crucibles were used for all samples, and preparation of the samples was conducted in an argon atmosphere dry box. The samples were prepared by removing a portion of the cathode electrode material from the Al current collector, obtaining an accurate mass of the cathode material (typically ca. 1 mg), and adding 3 μl of electrolyte (1.0 M $LiPF_6$ in 1:1 EC:DEC). The reference pan of the calorimeter contained an empty, sealed titanium crucible. To ensure reproducibility of the experimental data, multiple DSC curves were recorded for each sample.

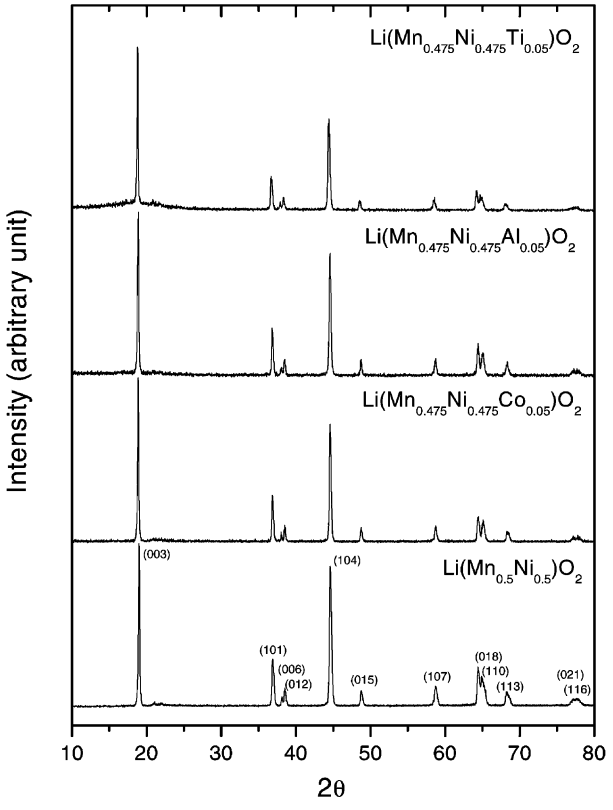

Fig. 1. Powder X-ray diffraction (XRD) patterns of $Li(Ni_{0.5-x}Mn_{0.5-x}M'_{2x})O_2$ ($M' = Co$, Al, Ti; $x = 0$, 0.025).

3. Results and discussion

3.1. Crystal structure and electrochemical analysis

The powder XRD patterns of $Li(Ni_{0.5-x}Mn_{0.5-x}M'_{2x})O_2$ ($M' = Co$, Al, Ti; $x = 0$, 0.025) are shown in Fig. 1. All of the peaks were indexed based on the α-$NaFeO_2$ structure ($R\bar{3}m$), which indicates that the synthesized samples were phase-pure and had a layered crystal structure.

In Fig. 2 are shown discharge curves of Li/$Li(Ni_{0.5-x}Mn_{0.5-x}M'_{2x})O_2$ ($M' = Co$, Al, Ti; $x = 0$, 0.025) cells cycled at 2.8–4.3 V; corresponding discharge capacities are given in Fig. 3. Discharge capacity of $Li(Ni_{0.5}Mn_{0.5})O_2$ was ca. 120 mAh/g with slight capacity fade (0.09% per cycle in average); M′-doped $Li(Ni_{0.5-x}Mn_{0.5-x}M'_{2x})O_2$ materials showed larger capacity than the $Li(Ni_{0.5}Mn_{0.5})O_2$ (140, 142, 132 mAh/g for $M' = Co$, Al, Ti, respectively) with excellent capacity retention.

The cyclic voltammogram (CV) of $Li(Ni_{0.5}Mn_{0.5})O_2$ sample is shown in Fig. 4. Unlike $LiNiO_2$, which exhibits three sharp peaks in the CV curves due to three distinct phase transitions [17], $Li(Ni_{0.5}Mn_{0.5})O_2$, upon charging, shows a major peak centered at ca. 4.0 V and a small, broad peak at ca. 4.4 V. All of the other materials exhibited similar CV to that of the $Li(Ni_{0.5}Mn_{0.5})O_2$. This observation suggests that multi-phase reactions during electrochemical cycling that leads to structural degradation as in $LiNiO_2$ are not present in $Li(Ni_{0.5-x}Mn_{0.5-x}M'_{2x})O_2$ materials. Furthermore, it is noted that no redox-reaction peaks are observed near 3 V in the CV. According to Paulsen et al. [18], Mn^{3+}/Mn^{4+} redox reactions occur at about 2.9 V in layer-structured $Li_{2/3}(Ni_{1/3}Mn_{2/3})O_2$. Therefore, the absence of the redox-reaction peaks in the 3 V region indicates that Mn ions are electrochemically inactive and are present in the +4 oxidation state in our samples. In a purely ionic scenario, most of the Ni ions must exist as Ni^{2+} in $Li(Ni_{0.5-x}Mn_{0.5-x}M'_{2x})O_2$ to maintain charge neutrality. Correspondingly, for example, $Li(Ni_{0.5}Mn_{0.5})O_2$ can be written as

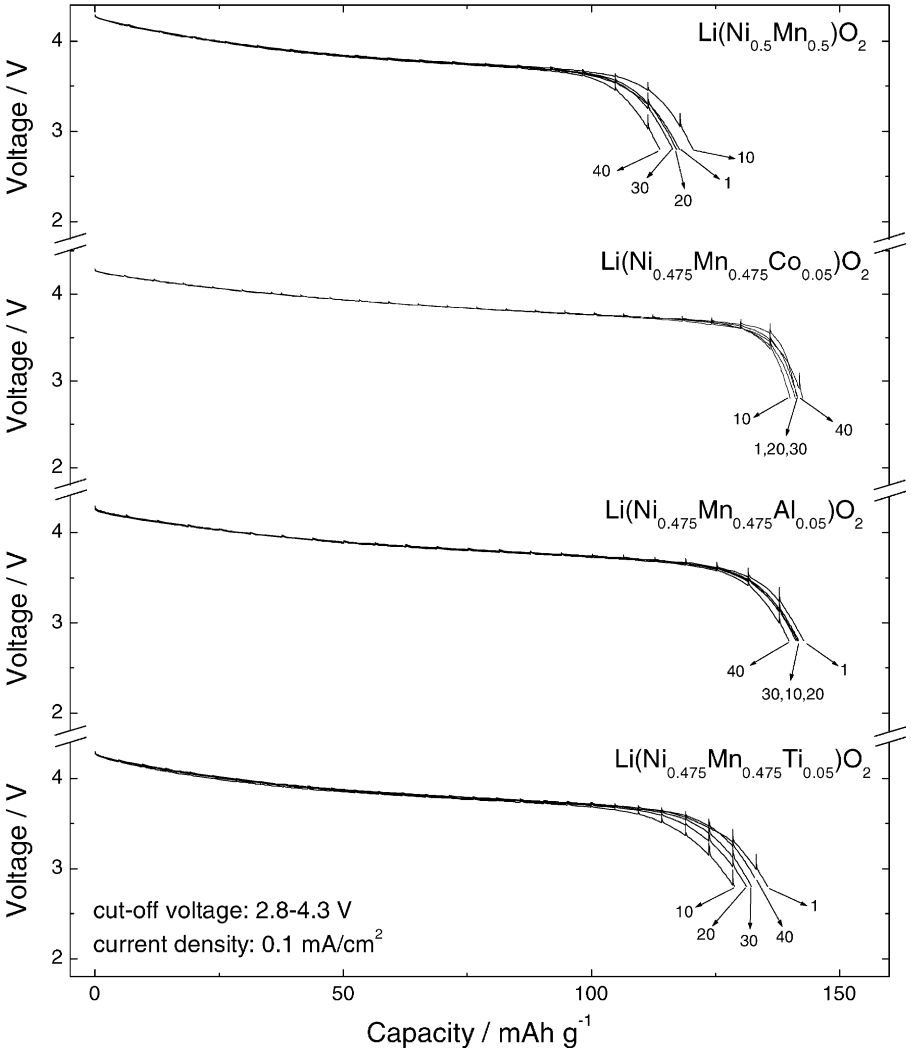

Fig. 2. Discharge curves of Li/$Li(Ni_{0.5-x}Mn_{0.5-x}M'_{2x})O_2$ ($M' = Co$, Al, Ti; $x = 0$, 0.025) cells in the voltage range of 2.8–4.3 V at a current density of 0.1 mA/cm^2.

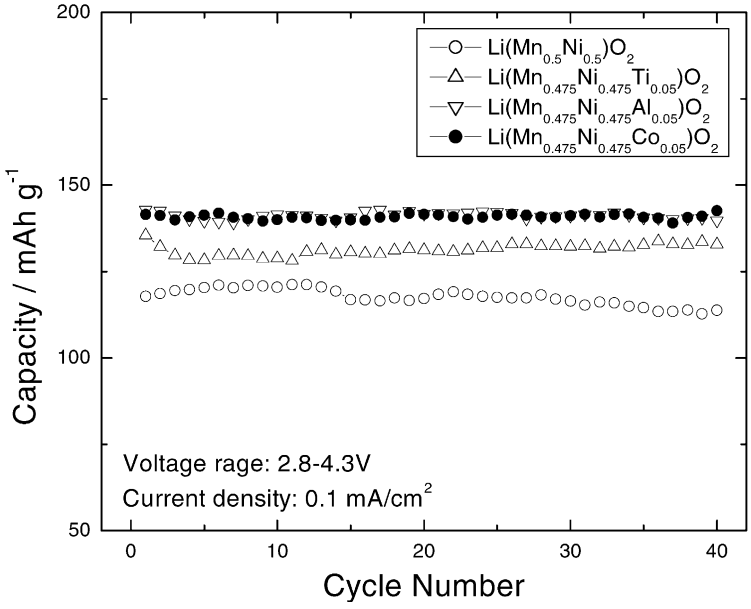

Fig. 3. Discharge capacities of $Li(Ni_{0.5-x}Mn_{0.5-x}M'_{2x})O_2$ (M′ = Co, Al, Ti; $x = 0$, 0.025) in the voltage range of 2.8–4.3 V at a current density of 0.1 mA/cm^2.

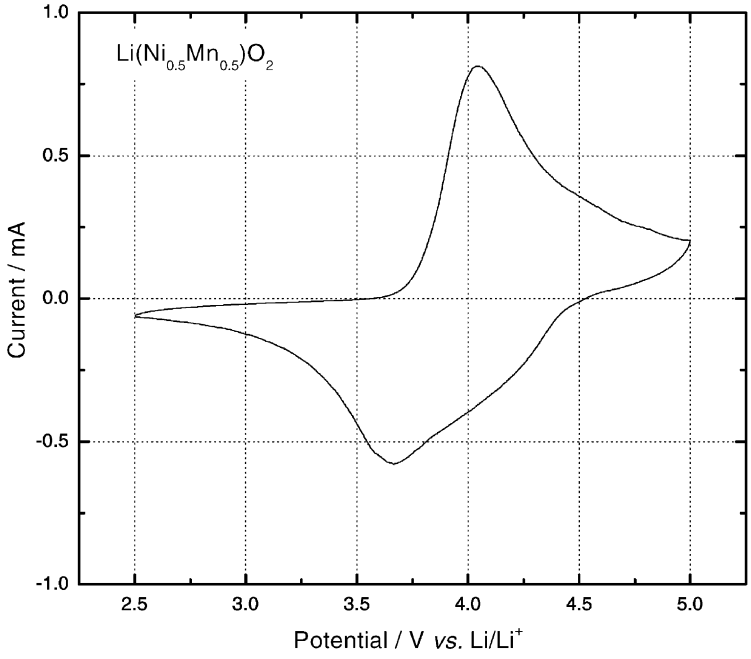

Fig. 4. Cyclic voltammetry profile of $Li(Ni_{0.5}Mn_{0.5})O_2$ at a sweep rate of 100 μV/s.

$Li(Ni_{0.5}{}^{2+}Mn_{0.5}{}^{4+})O_2$. The presence of Ni as Ni^{2+} in layered oxides containing Mn and Co has also been proposed by other investigators [16,18,19]. The peaks centered at ~4 V in the CV are, therefore, attributed to the redox reactions of Ni^{2+}/Ni^{3+} and/or Ni^{2+}/Ni^{4+} as was speculated by Lu et al. [16].

3.2. Oxidation states of Ni and Mn in $Li(Ni_{0.5}Mn_{0.5})O_2$

To determine the oxidation states of Ni and Mn in the layered materials, XPS experiments were carried out for $Li(Ni_{0.5}Mn_{0.5})O_2$; the XPS spectra of Mn 3p, Mn $2p_{3/2}$, and

Table 1
Electron binding energies of $Li(Ni_{0.5}Mn_{0.5})O_2$ and reference oxides

Compound	Binding energy (eV)			Reference
	Mn $2p_{3/2}$	Mn 3p	Ni $2p_{3/2}$	
$Li(Ni_{0.5}Mn_{0.5})O_2$	642.1	49.8	854.3	This work
NiO			854.1	This work
Ni_2O_3			855.2	This work
$LiNiO_2$			855.4	[20]
$Li_2Mn_2O_4$	641.4	48.5		[21]
λ-MnO_2	642.4	49.7		[21]

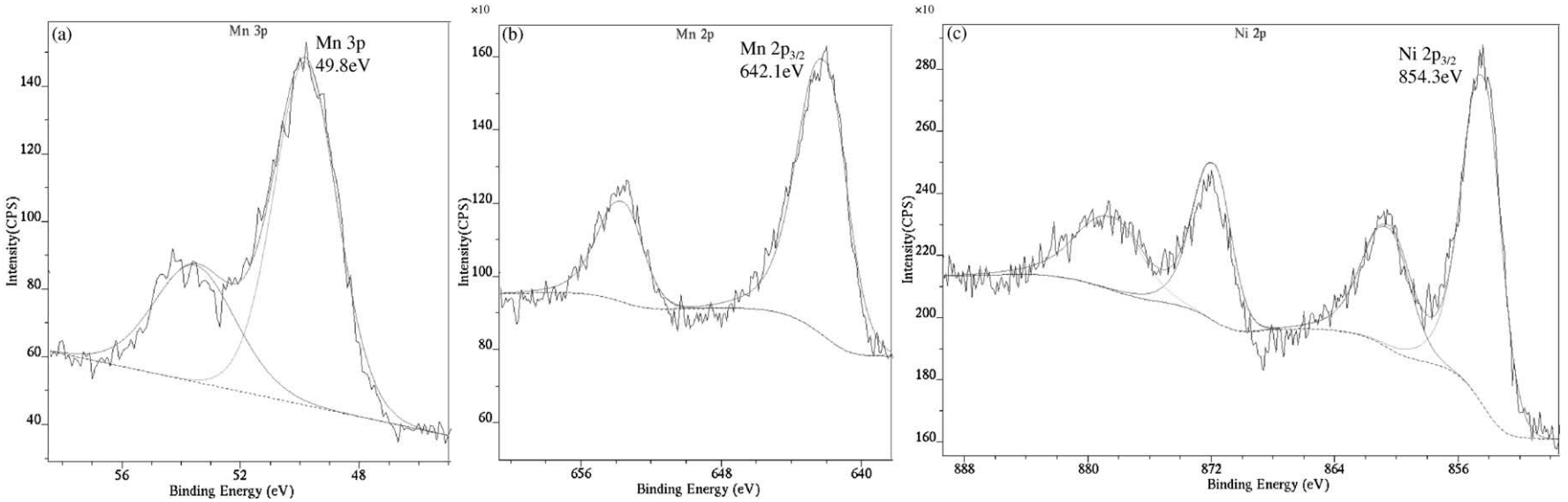

Fig. 5. X-ray photoelectron spectroscopy (XPS) spectra of: (a) Mn 3p, (b) Mn $2p_{3/2}$, and (c) Ni $2p_{3/2}$ for $Li(Ni_{0.5}Mn_{0.5})O_2$.

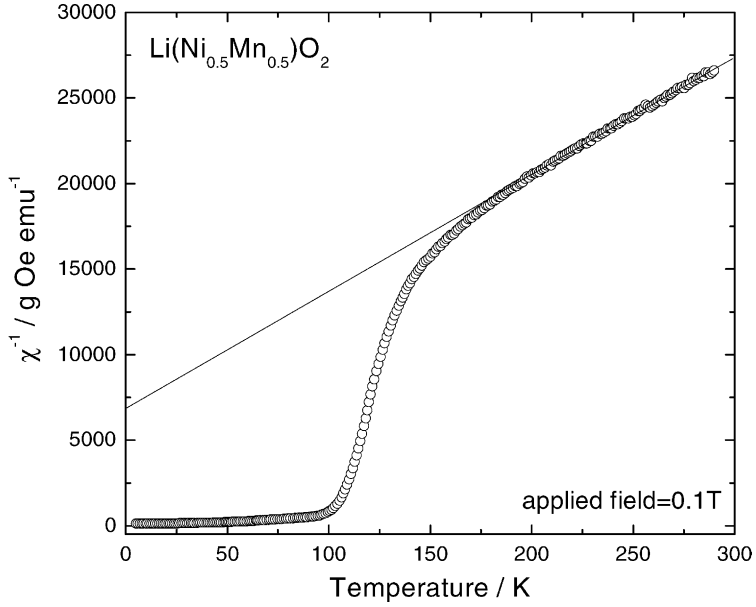

Fig. 6. The inverse magnetic susceptibility of $Li(Ni_{0.5}Mn_{0.5})O_2$ between 5 and 300 K at an applied field of 0.1 T.

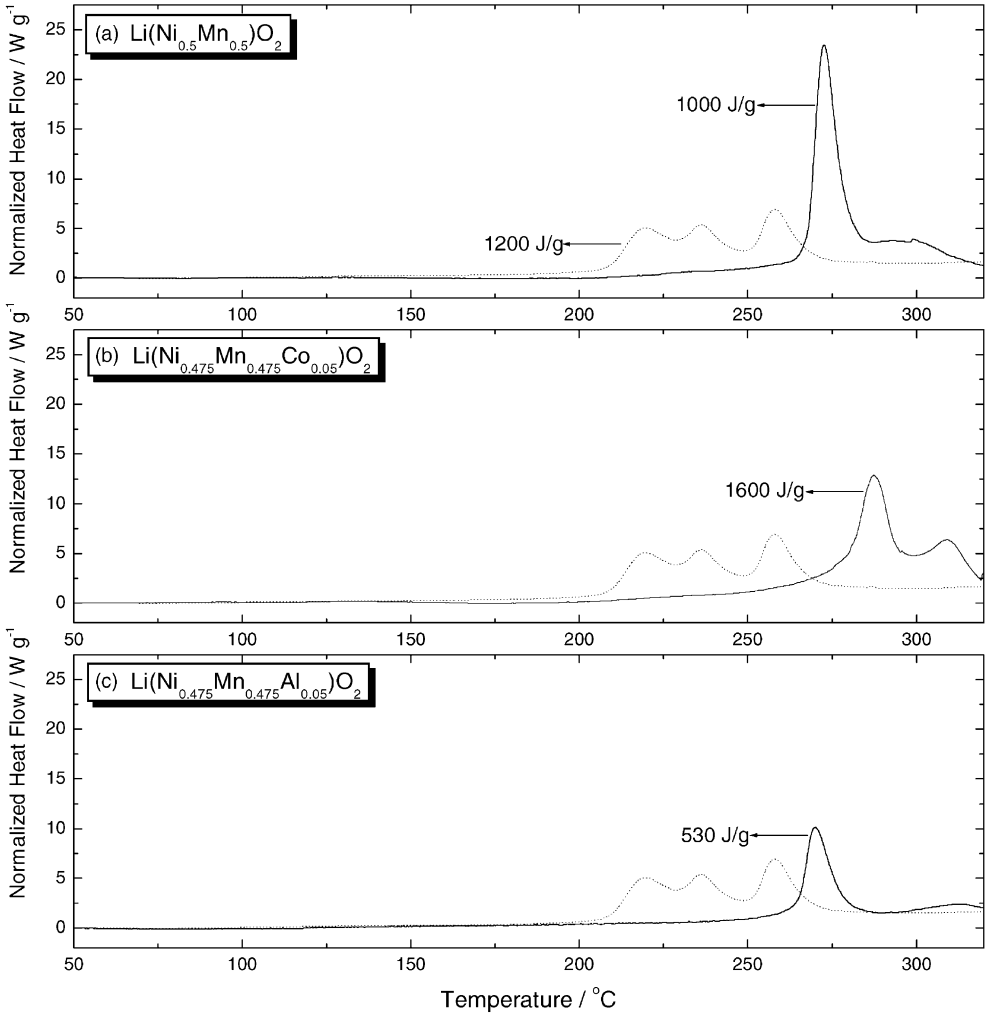

Fig. 7. Differential scanning calorimetry (DSC) profile (10 °C/min) of: (a) $Li(Ni_{0.5}Mn_{0.5})O_2$, (b) $Li(Ni_{0.475}Mn_{0.475}Co_{0.05})O_2$, and (c) $Li(Ni_{0.475}Mn_{0.475}Al_{0.05})O_2$ charged to 4.3 V. DSC profile of $Li(Ni_{0.80}Co_{0.20})O_2$ (dotted lines) charged to 4.2 V was taken from [24] for comparison.

Ni $2p_{3/2}$ for $Li(Ni_{0.5}Mn_{0.5})O_2$ are given in Fig. 5, and the electron binding energies of reference compounds are listed in Table 1. In $Li(Ni_{0.5}Mn_{0.5})O_2$, the Ni $2p_{3/2}$ peak is at 854.3 eV, which is similar to the binding energy of Ni^{2+} in NiO. The Mn $2p_{3/2}$ peak is at 642.1 eV, which is closer to the value measured for Mn^{4+} in λ-MnO_2 than for Mn^{3+} in $Li_2Mn_2O_4$. Furthermore, the Mn 3p peak at 49.8 eV is similar to that measured for Mn^{4+} in λ-MnO_2. These data suggest that Ni and Mn ions are present as Ni^{2+} and Mn^{4+}, respectively, which is consistent with the CV results. However, the XPS spectra are characteristic of the sample surfaces; other experiments, such as X-ray absorption spectroscopy (XAS), are necessary to determine the elemental oxidation states in the bulk sample.

Temperature-dependent magnetic susceptibility measurement is another experimental technique generally adopted to estimate oxidation states of transition metal ions because the magnetic moment of ions is dependent on their spin state [22,23]. The temperature-dependent magnetic susceptibility of $Li(Ni_{0.5}Mn_{0.5})O_2$ is shown in Fig. 6 where the $Li(Ni_{0.5}Mn_{0.5})O_2$ sample exhibited the Curie–Weiss behavior between 180 and 300 K with a paramagnetic Curie temperature of −92 K and magnetic moment of 3.4 μ_B. Spahr et al. [20] reported similar results for the same material (−107 K and 3.3 μ_B), and they claimed that the magnetic moment was in good agreement with the calculated value for $Li(Ni_{0.5}{}^{3+}Mn_{0.5}{}^{3+})O_2$ (3.32 μ_B). However, the calculated magnetic moment of $Li(Ni_{0.5}{}^{2+}Mn_{0.5}{}^{4+})O_2$ is 3.35 μ_B, which differs by less than 1% from that of $Li(Ni_{0.5}{}^{3+}Mn_{0.5}{}^{3+})O_2$. Consequently, it is very difficult to determine conclusively the oxidation states of Ni and Mn in $Li(Ni_{0.5}Mn_{0.5})O_2$ by the magnetic moment measurements.

3.3. Differential scanning calorimetry

Differential scanning calorimetry profiles of $Li(Ni_{0.5-x}Mn_{0.5-x}M'_{2x})O_2$ samples charged to 4.3 V in Li/$Li(Ni_{0.5-x}Mn_{0.5-x}M'_{2x})O_2$ cells are given in Fig. 7; data from $Li(Ni_{0.80}Co_{0.20})O_2$ charged to 4.2 V [24] are also shown for comparison. $Li(Ni_{0.5}Mn_{0.5})O_2$ exhibited one sharp exothermic peak at 272 °C with an onset temperature of 268 °C and 1050 J/g of heat associated with the exothermic peak, whereas $Li(Ni_{0.80}Co_{0.20})O_2$ showed three distinct exothermic peaks with an onset temperature of 200 °C and 1240 J/g of total heat associated with the three peaks. The DSC curve of $Li(Ni_{0.475}Mn_{0.475}Co_{0.05})O_2$ consists of two different peaks: one is at 290 °C with an onset temperature of 280 °C and the other is at 310 °C. Total heat associated with the two exothermic peaks was 1270 J/g. The $Li(Ni_{0.475}Mn_{0.475}Al_{0.05})O_2$ material showed a similar DSC curve to that of $Li(Ni_{0.5}Mn_{0.5})O_2$ in terms of peak position and onset temperature but with a much smaller amount of heat (530 J/mol) than the other materials. Consequently, $Li(Ni_{0.5-x}Mn_{0.5-x}M'_{2x})O_2$ materials have better thermal safety characteristics than the $LiNiO_2$-based cathode materials as shown in Fig. 7 and in literature [8].

3.4. Area specific impedance

Area specific impedance (ASI) is directly related to power capability of a battery and it should be lower than 35 Ω cm^2 to meet the Partnership for a New Generation of Vehicles (PNGV) requirement for the battery to power an HEV [25]. Fig. 8 shows the ASI as a function of state of charge (SOC) measured with $C/Li(Ni_{0.5-x}Mn_{0.5-x}M'_{2x})O_2$ (M′ = Co, Al, Ti; $x = 0, 0.025$) cells. The ASI was determined by $(A\ \Delta V)/I$,

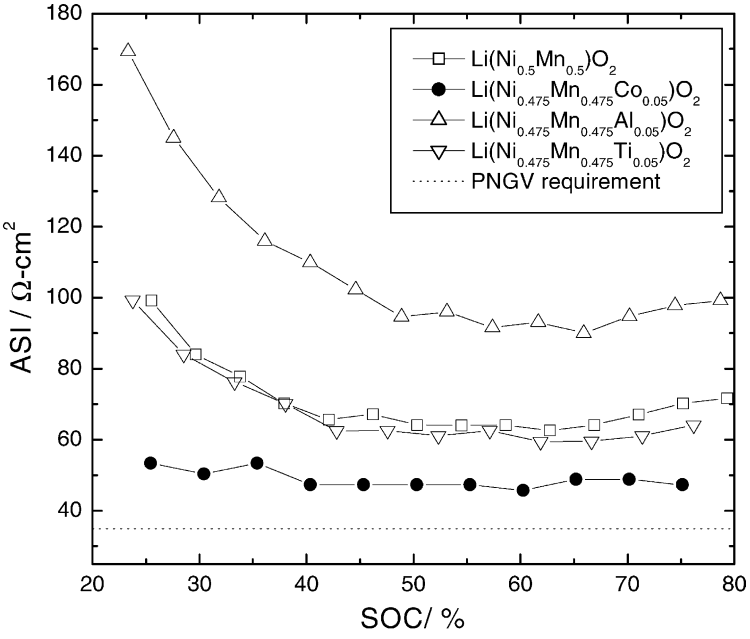

Fig. 8. Area specific impedance (ASI) of $C/Li(Ni_{0.475}Mn_{0.475}M'_{0.05})O_2$ cells as a function of state of charge (SOC).

where A is the cross-sectional area, ΔV the voltage variation during current interruption for 30 s at each SOC, and I the current applied during the galvanostatic cycling. $Li(Ni_{0.5}Mn_{0.5})O_2$ exhibited an ASI value of 64 $\Omega\,cm^2$ at 40–60% SOC, which is higher than the PNGV requirement. Whereas $Li(Ni_{0.475}Mn_{0.475}Ti_{0.05})O_2$ and $Li(Ni_{0.475}Mn_{0.475}Al_{0.05})O_2$ showed similar or higher ASI values (62 and 99 $\Omega\,cm^2$, respectively), $Li(Ni_{0.475}Mn_{0.475}Co_{0.05})O_2$ exhibited a smaller ASI value (47 $\Omega\,cm^2$) than the undoped sample although it is still higher than the PNGV requirements. The decrease of ASI values with the 5 mol% Co-doping is partly attributed to the enhancement of electrical conductivity of the material: preliminary studies revealed that the electrical conductivity increased by two orders of magnitude with 5 mol% Co-doping (2.5×10^{-6} and $2.3 \times 10^{-4}\ \Omega^{-1}\,cm^{-1}$ for $Li(Ni_{0.5}Mn_{0.5})O_2$ and $Li(Ni_{0.475}Mn_{0.475}Co_{0.05})O_2$, respectively). Various efforts are being made to lower the ASI values below 35 $\Omega\,cm^2$ through optimization of various factors, such as nature and content of doping elements, morphology of oxide powders, and the quantity of carbon and binder in the cathode. The success in lowering the ASI of these materials to meet the PNGV power requirement will make those materials very attractive for application in HEV batteries because they are of lower cost and could provide batteries with long calendar life and enhanced safety.

4. Summary and conclusions

Layered $Li(Ni_{0.5-x}Mn_{0.5-x}M'_{2x})O_2$ ($M' = Co$, Al, Ti; $x = 0$, 0.025) materials were synthesized using a manganese-nickel hydroxide as a precursor. $Li(Ni_{0.5}Mn_{0.5})O_2$ delivered a discharge capacity of 120 mAh/g at 2.8–4.3 V. The discharge capacity of the materials increased by 10–20% and capacity retention was improved by doping with 5 mol% Co, Al, or Ti. Cyclic voltammograms of all of the materials showed one major redox peak, which suggests that structural phase transitions are not present during the electrochemical cycling. The cyclic voltammetry and X-ray photoelectron spectroscopy data suggest that Ni and Mn are present in $Li(Ni_{0.5-x}Mn_{0.5-x}M'_{2x})O_2$ samples as Ni^{2+} and Mn^{4+}, respectively. Differential scanning calorimetry experiments revealed that $Li(Ni_{0.5-x}Mn_{0.5-x}M'_{2x})O_2$ has better thermal safety characteristics than $LiNiO_2$-based cathode materials.

In conclusion, $Li(Ni_{0.5-x}Mn_{0.5-x}M'_{2x})O_2$ are good candidates for cathode materials of rechargeable lithium-ion batteries for hybrid electric vehicle applications in terms of capacity, stability, and thermal safety. But impedance of the materials still needs to be improved to meet the PNGV requirements. Extensive studies are under way to reduce the impedance of the materials.

Acknowledgements

This work was supported by the US Department of Energy, Office of Advanced Automotive Technologies, under Contract No. W-31-109-ENG-38. The XPS experiments were conducted at the Center for Microanalysis of Materials, University of Illinois; this facility is supported by the US Department of Energy under grant DEFG02-96-ER45439. We acknowledge Dr. Rick Haasch for his assistance with acquiring and processing the XPS data.

References

[1] I. Davidson, J.E. Greedan, U. von Sacken, C.A. Michal, J.R. Dahn, Solid State Ionics 46 (1991) 243.
[2] G. Dutta, A. Manthiram, J.B. Goodenough, J. Solid State Chem. 96 (1992) 123.
[3] T. Ohzuku, A. Ueda, M. Nagayama, J. Electrochem. Soc. 140 (1993) 1862.
[4] T. Ohzuku, A. Ueda, T. Hirai, Chem. Express 7 (1992) 193.
[5] R.J. Gummow, D.C. Liles, M.M. Thackeray, Mater. Res. Bull. 28 (1993) 1249.
[6] A.R. Armstrong, P.G. Bruce, Nature 381 (1996) 499.
[7] T. Ohzuku, A. Ueda, M. Kouguchi, J. Electrochem. Soc. 142 (1995) 4033.
[8] Y. Gao, M.V. Yakovleva, W.B. Ebner, Electrochem. Solid-State Lett. 1 (1998) 117.
[9] D. Caurant, N. Baffier, B. Garcia, J.P. Pereira-Ramos, Solid State Ionics 91 (1996) 45.
[10] M. Yoshio, Y. Todorov, K. Yamato, H. Noguchi, J. Itoh, M. Okada, T. Mouri, J. Power Sources 74 (1998) 46.
[11] J. Kim, K. Amine, Electrochem. Commun. 3 (2001) 52.
[12] G. Vitins, K. West, J. Electrochem. Soc. 144 (1997) 2587.
[13] Y.-I. Jang, B. Huang, Y.-M. Chiang, D.R. Sadoway, Electrochem. Solid-State Lett. 1 (1998) 13.
[14] J.M. Paulsen, C.L. Thomas, J.R. Dahn, J. Electrochem. Soc. 146 (1999) 3560.
[15] T. Ohzuku, Y. Makimura, Chem. Lett. (2001) 744.
[16] Z. Lu, D.D. MacNeil, J.R. Dahn, Electrochem. Solid-State Lett. 4 (2001) A191.
[17] W. Li, J.N. Reimers, J.R. Dahn, Solid State Ionics 67 (1993) 123.
[18] J.M. Paulsen, C.L. Thomas, J.R. Dahn, J. Electrochem. Soc. 147 (2000) 861.
[19] L.A. Montoro, M. Abbate, J.M. Rosolen, J. Electrochem. Soc. 147 (2000) 1651.
[20] M.E. Spahr, P. Novak, B. Schnyder, O. Haas, R. Nespar, J. Electrochem. Soc. 145 (1998) 1113.
[21] T. Eriksson, Ph.D. Thesis, Uppsala University, Uppsala, Sweden, 2001.
[22] Y. Nitta, K. Okamura, K. Haraguchi, S. Kobayashi, A. Ohta, J. Power Sources 54 (1995) 511.
[23] J.E. Greedan, N.P. Raju, J. Solid State Chem. 128 (1997) 209.
[24] C.H. Chen, J. Liu, M.E. Stoll, K. Amine, in preparation.
[25] PNGV Battery Test Manual, Revision 1, Idaho National Engineering Laboratory, Department of Energy, DOE/ID-10597, May 1998.